arXiv:cond-mat/9804195v1 [cond-mat.mtrl-sci] 17 Apr 1998

Effective electronic response of a system of metallic cylinders

J. M. Pitarke[1], F. J. García-Vidal[2], and J. B. Pendry[3]

[1]*Materia Kondentsatuaren Fisika Saila, Zientzi Fakultatea, Euskal Herriko Unibertsitatea, 644 Posta kutxatila, 48080 Bilbo, Basque Country, Spain*

[2]*Departamento de Física Teórica de la Materia Condensada, Facultad de Ciencias, Universidad Autónoma de Madrid, 28049 Madrid, Spain*

[3]*Condensed Matter Theory Group, The Blacket Laboratory, Imperial College, London SW7 2BZ, United Kingdom*

(March 9 1998)

Abstract

The electronic response of a composite consisting of aligned metallic cylinders in vacuum is investigated, on the basis of photonic band structure calculations. The effective long-wavelength dielectric response function is computed, as a function of the filling fraction. A spectral representation of the effective response is considered, and the surface mode strengths and positions are analyzed. The range of validity of a Maxwell-Garnett-like approach is discussed, and the impact of our results on absorption spectra and electron energy-loss phenomena is addressed.

Typeset using REVTEX

I. INTRODUCTION

Both theoretical and experimental investigations of the optical properties of composite materials have been of basic importance over the years[1]. In particular, effective medium theories, in which the electromagnetic response of the composite is described in terms of an effective dielectric function ϵ_{eff}, have been a useful tool for the interpretation of absorption spectra[2]. Mean-field theories of the effective response function have also been proved to be useful to analyze electron energy-loss experiments in which swift electrons penetrate composites at random distances from the particles[3−9].

In the long-wavelength limit, the effective transverse dielectric function for a system of spherical particles was first derived by Maxwell-Garnett (MG)[10], within a mean-field approximation valid for small values of the volume occupied by the spheres. A generalization of the MG theory to finite wavelength, taking account of the spatial nonlocality in the response, has been recently presented by Barrera and Fuchs[7]. On the other hand, many attempts have been made to account, at large filling fractions, for higher multipole interactions, which are absent in the MG theory[11−15]. Recently, exact numerical calculations for periodic dielectric structures have been performed[16], based in the long-wavelength limit of photonic band structure calculations, and the MG theory has been shown to offer a good approximation in the low-filling-ratio regime. Finally, the discovery of tubular fullerenes[17], a few years ago, has opened a new focus of interest for the application of these theories to the case of cylindrical interfaces[18,19].

In this paper we evaluate, on the basis of photonic band structure calculations, the long-wavelength limit of the effective transverse dielectric function of a composite made up of long metallic cylinders embedded in an otherwise homogeneous medium. We first demonstrate that the composite can be replaced by an effective homogeneous medium, and then we determine the transverse dielectric function of that medium from the electromagnetic modes supported by such a homogeneous system. We consider a spectral representation of the effective dielectric function, we present an evaluation of the parameters involved, and

we discuss the range of validity of a MG-like approach appropriate for cylindrical particles. We also address the impact of our results on absorption spectra and electron energy-loss phenomena.

II. THEORY

It was shown by Bergman[21] and Milton[22] that in the long-wavelength limit the effective dielectric function of any macroscopically homogeneous two-component system of dielectric constants ϵ and ϵ_0 and volume fractions f and $1-f$, respectively, can be expressed as a sum of simple poles which depend only on the microgeometry of the composite material and not on the dielectric functions of the components:

$$\epsilon_{\text{eff}} = \epsilon_0 \left[1 - f \sum_{\nu} \frac{B_\nu}{u - m_\nu} \right], \tag{1}$$

where u is the spectral variable

$$u = \left[1 - \epsilon/\epsilon_0 \right]^{-1}, \tag{2}$$

m_ν are depolarization factors, and B_ν are the strengths of the corresponding normal modes, which all add up to unity:

$$\sum_{\nu} B_\nu = 1. \tag{3}$$

Similarly[23],

$$\epsilon_{\text{eff}}^{-1} = \epsilon_0^{-1} \left[1 - f \sum_{\nu} \frac{C_\nu}{u - n_\nu} \right] \tag{4}$$

and

$$\sum_{\nu} C_\nu = 1. \tag{5}$$

In particular, if there is only one mode with a strength different from zero, one finds:

$$\epsilon_{\text{eff}}(\omega) = \epsilon_0 \left[1 - f \frac{1}{u - m_1} \right] \tag{6}$$

and

$$\epsilon_{\rm eff}^{-1}(\omega) = \epsilon_0^{-1}\left[1 + f\frac{1}{u - n_1}\right]. \tag{7}$$

We consider a binary composite with a volume fraction $1 - f$ of insulator, with real dielectric constant ϵ_0, and f of a periodic system of long metallic cylinders of diameter d arranged in a square array with lattice constant $a = x\,d$ (See Fig. 1). The diameter of the cylinders is taken to be small in comparison with the wavelength of the electromagnetic excitation and large enough that a macroscopic dielectric function $\epsilon(\omega)$ is ascribable to the cylinders. For simplicity, the magnetic permeabilities are assumed to be equal to unity in both media.

Now we take an electromagnetic (EM) wave normally incident on the structure, so that $k_x = k_y = 0$. For this propagation direction there are two different values of $\epsilon_{\rm eff}(\omega)$ corresponding to different polarizations. In the case of EM waves polarized along the cylinders (s polarization), the presence of the interfaces does not modify the electric field, and one easily finds[24] that the response of the composite is equivalent to that of a homogeneous medium having the effective transverse dielectric function of Eqs. (6) and (7) with $m_1 = 0$ and $n_1 = f$.

For EM waves polarized normal to the cylinders (p polarization), we first consider the case of a single cylinder embedded in an otherwise homogeneous medium. An elementary analysis of this classical problem shows that the electric field in the interior of the cylinder is[25]

$$\mathbf{E}_{\rm in} = \frac{u}{u - 1/2}\mathbf{E}_{\rm out}, \tag{8}$$

where $\mathbf{E}_{\rm out}$ represents the electric field intensity in the medium outside the cylinder. The effective dielectric function of isolated cylinders is then found to be given, again, by Eqs. (6) and (7), the depolarization factors now being $m_1 = n_1 = 1/2$. In the case of isolated particles only the dipole surface mode enters Eqs. (1) and (4) for this polarization.

The interaction between the particles in a composite has been considered, over the years, within the well-known MG approximation. The basic assumption of this approach is that

the average electric field within a particle located in a system of identical particles is related to the average field in the medium outside as in the case of a single isolated particle, thus only dipole interactions being taken into account. Hence, after replacing, for p polarization, $\mathbf{E}_{\rm out}$ of Eq. (8) by

$$\mathbf{E}_{\rm out} = \frac{< \mathbf{E} > - f\mathbf{E}_{\rm in}}{1-f}, \tag{9}$$

$< \mathbf{E} >$ being the macroscopic effective electric field in the composite, the MG result for cylindrical inclusions is found, which can be represented by the use of Eqs. (6) and (7) with

$$m_1 = \frac{1}{2}(1-f) \tag{10}$$

and

$$n_1 = \frac{1}{2}(1+f). \tag{11}$$

This is a special case of the generalized MG dielectric function derived in Ref. 25 for ellipsoidal inclusions, which in the case of aligned spheroids distributed at random has been extended beyond the MG approximation[26]. Higher multipole interactions are neglected in these approaches.

In order to compute, with full inclusion of higher multipoles, the effective dielectric function of our periodic system, we first follow Ref. 20 to calculate the photonic band structure. We fix the frequency, the local dielectric function inside the cylinders being therefore specified, and we discretize the Maxwell equations within the unit cell. The discretized Maxwell equations provide a relationship between the electromagnetic fields on either side of the unit cell, i.e., z and $z+a$ (see Fig. 1), and we exploit this to calculate, on applying Bloch's theorem, the eigenvalues of the so-called transfer matrix, which will give the band structure of the system.

Homogeneous media are well known to support only two transverse modes. On the other hand, looking at the imaginary part of the eigenvalues of the system, we observe that over the entire range of frequencies there are, for each polarization, two degenerate EM Bloch waves

with vectors k and $-k$ for which $k(\omega)$ roughly follows the dispersion relation of free light and which are dominant in the sense that they present the smallest attenuation (smallest imaginary part of k). Thus, we conclude that the composite can be replaced by an effective homogeneous medium, and we use the dispersion relation of these Bloch waves to compute the effective transverse dielectric function from

$$\epsilon_{\text{eff}}(\omega) = \frac{k^2 c^2}{\omega^2}, \tag{12}$$

where c is the speed of light.

III. RESULTS AND DISCUSSION

We have taken the insulating component of the composite to have a real dielectric constant of $\epsilon_0 = 1$, and we have modeled the dielectric properties of the metal inside the cylinders by a simple free-electron (Drude) dielectric function:

$$\epsilon(\omega) = 1 - \frac{\omega_p^2}{\omega(\omega + \mathrm{i}\gamma)}, \tag{13}$$

where ω_p is the bulk plasma frequency of the metal, and γ represents an inverse electron relaxation time. We have used the plasma frequency of the conduction electrons in Aluminum, $\hbar\omega_p = 15.8\text{eV}$, and $\gamma = 1.4\text{eV}$.

For s polarized electromagnetic waves, our numerical results for the effective dielectric function, as obtained from Eq. (12), accurately reproduce the exact results of Eq. (6) and (7) with $m = 0$ and $n = f$, and this represents, therefore, a good check of our scheme.

In the case of p polarized electromagnetic excitations, great care was exercised to ensure that our calculations are insensitive to the precise value of the number of mesh points in the unit cell[27]. The results presented below have been found to be well-converged for all filling fractions, and they all correspond to a sampling mesh of $180 \times 1 \times 180$[28].

The optical absorption is directly given by the imaginary part of the effective dielectric function, $\text{Im}\,[\epsilon_{\text{eff}}(\omega)]$. Thus, for p polarization the absorption spectra of isolated cylinders

($f \to 0$) exhibit a strong maximum, absent in the bulk metal, at the cylinder dipole resonance ($\epsilon(\omega) + \epsilon_0 = 0$), i.e., at $\omega_1 = \sqrt{m_1}\omega_p$ with $m_1 = 1/2$. At higher concentrations of metal, $\mathrm{Im}\left[\epsilon_{\mathrm{eff}}(\omega)\right]$ still shows a dipole resonance at $\omega_1 = \sqrt{m_1(f)}\omega_p$ ($m_1(f) \neq 1/2$), and a band of multipole resonances at $\omega_\nu = \sqrt{m_\nu(f)}\omega_p$ ($\nu = 2, \ldots ; m_\nu > m_1$) is also formed broadened by electromagnetic interactions among individual cylinders. This is illustrated in Fig. 2, where our first principles calculations of $\mathrm{Im}\left[\epsilon_{\mathrm{eff}}(\omega)\right]/f$ are exhibited, as a function of the frequency ω, for various values of the ratio x between the lattice constant and the diameter of the cylinders. For $x \geq 2$ the effective dielectric function is well described by the MG approximation, and both our computed result and the MG approximation almost coincide for $x = 6$ with the isolated cylinder result, represented in Fig. 2 by a thin solid line. In Fig. 3 our results are compared, for two different filling fractions, with the MG approximation, showing that together with the appearance of multipole resonances the depolarization factors $m_1(f)$ are, for $x < 2$, smaller than the MG depolarization factor of Eq. (10).

In the case of a broad beam of charged particles penetrating the composite, the probability per unit path length, per unit energy, for the projectile to transfer energy $\hbar\omega$ to the medium is[29]

$$P_\omega = \frac{2e^2}{\hbar^2 v^2} F(\omega), \tag{14}$$

where

$$F(\omega) = \frac{1}{\pi}\int_0^{Q_c} \mathrm{d}Q \frac{Q}{Q^2 + q_v^2} \mathrm{Im}\left[-\epsilon_{eff}^{-1}(\mathbf{q},\omega)\right], \tag{15}$$

$\mathbf{v}$ and $\epsilon_{eff}^{-1}(\mathbf{q},\omega)$ being the velocity of the incident particles and the effective inverse longitudinal dielectric function of the composite, respectively. $\hbar\mathbf{Q}$ represents the component of the momentum transfer, $\hbar\mathbf{q}$, located in a plane perpendicular to the incident beam direction, Q_c is determined by $q_c^2 = Q_c^2 + q_v^2$, q_c representing the largest wave vector for which plasmons are well-defined excitations[30], and

$$q_v = \frac{\omega}{v}. \tag{16}$$

In typical electron energy-loss experiments swift electrons of about 100keV penetrate the composite, and the main contribution to the integral of Eq. (15) comes, therefore, from very small values of the momentum transfer. Also, for small values of the adimensional parameter qa ($qa < 1$), a being the radius of the cylinder, the effective dielectric function of isolated cylinders has been proved to be rather insensitive to the introduction of a finite wave vector[9,29], and the energy-loss spectra of swift electrons is therefore expected to be, for small values of the radius of the cylinders ($a < 1$nm)[31], well described by the $q \to 0$ limit of the imaginary part of the effective inverse dielectric function[32].

Eq. (7) with $n = 0$ (dilute limit of $n = f$) and $n = 1/2$ exactly coincides, in the long-wavelength limit, with the result one obtains for the effective inverse longitudinal dielectric function of isolated cylinders when the momentum transfer is parallel to the axis and when it is located in a plane perpendicular to the axis of the cylinder, respectively[29]. In this limit ($q \to 0$) bulk plasmons are not excited, as a consequence of the so-called Bregenzung effect, and the pole in Eq. (7) at $\epsilon(\omega) + \epsilon_0 = 0$, i.e., $\omega_1 = \sqrt{m_1}\omega_p$ with $m_1 = 1/2$, determines, for p polarization, the frequency of the so-called surface plasmon resonance at which electron energy-loss occurs.

Fig. 4 shows, as a function of the frequency, our calculations of $\mathrm{Im}[-\epsilon_{\mathrm{eff}}^{-1}(\omega)]/f$ obtained for various filling fractions by varying the ratio x between the lattice constant and the diameter of the cylinders. In a homogeneous metal the so-called energy-loss function, $\mathrm{Im}[-\epsilon_{\mathrm{eff}}^{-1}(\omega)]$, shows a single peak at the bulk plasmon resonance, and this peak persists in the composite for $x \leq 1$, i.e., for filling fractions of metal for which the insulator no longer forms a connected medium. Besides this peak, there is also a band in $\mathrm{Im}[-\epsilon_{\mathrm{eff}}^{-1}(\omega)]$ from multipole contributions to the effective response at $\omega_\nu = \sqrt{n_\nu(f)}\omega_p$ ($\nu = 2, \ldots$; $n_\nu < n_1$). As in the case of $\mathrm{Im}\,[\epsilon_{\mathrm{eff}}(\omega)]$, the energy-loss function is well described by the MG approximation in the low-filling-ratio regime, and our results begin to deviate from those obtained within the MG approximation at $x \approx 2$ (see Fig. 5). We also find that the depolarization factors $n_1(f)$ are larger than the MG depolarization factor of Eq. (11) for all volume fractions of metal for which the MG theory does not reproduce our results.

Our numerical calculations of the effective dielectric function, as obtained from Eq. (12), lead us to the conclusion that the depolarization factors m_1 and n_1 of Eqs. (1) and (4), corresponding to dipolar modes, satisfy the following relation:

$$n_1 = 1 - (D-1)m_1, \tag{17}$$

where D represents the dimensionality of the inclusions, i.e., $D = 3$ in the case of spherical inclusions and $D = 2$ in the case of long circular cylinders. If all multipolar modes are neglected, then $B_1 = C_1 = 1$ in Eqs. (1) and (4) and a combination of these equations with Eq. (17) results, for $D = 2$, in the spectral representations of Eqs. (6) and (7) with the depolarization factors m_1 and n_1 given by Eqs. (10) and (11), i.e., the MG approximation. On the other hand, as long as multipolar modes give non-negligible contributions to the spectral representation of the effective response, i.e., $B_\nu \neq 0$ and $C_\nu \neq 0$ ($\nu = 2, ...$), the strengths of the dipolar modes, B_1 and C_1, become smaller than unity (see Eqs. (3) and (5)), and a combination of Eqs. (1) and (4) with Eq. (17) leads us to the conclusion that the depolarization factors n_1 and m_1 necessarily deviate from their MG counterparts. That a non-vanishing contribution from multipolar modes appears together with a deviation of the dipolar mode locations with respect to their MG counterparts is apparent from Figs. 3 and 5.

One of the main advantages of the spectral representation of Eqs. (1) and (4) is that the depolarization factors and the strengths of the corresponding normal modes depend only on the microgeometry of the composite material and not on the dielectric function of the components. On the other hand, the normal mode positions are determined by m_ν and n_ν, and we have thus represented in Fig. 6, in the case of p polarization, universal curves for the actual dipolar mode depolarization factors and strengths versus the filling fraction. It is obvious from this figure that the trend with increasing filling fraction is for the dipolar peaks in $\mathrm{Im}\left[\epsilon_{\mathrm{eff}}(\omega)\right]$ / $\mathrm{Im}\left[-\epsilon_{\mathrm{eff}}^{-1}(\omega)\right]$ to move from the cylinder dipole mode ($m_1 = n_1 = 1/2$) to lower / higher energies. Notice that the MG results, also plotted in this figure, agree with our numerical results for $f < 0.2$ ($x > 2$). Nevertheless, at higher filling fractions the

actual depolarization factors approach more rapidly, as f is increased, the depolarization factors appropriate to the homogeneous metal ($m_1 = 0$ and $n_1 = 1$). In particular, for $x < 1$ ($f > \pi/4$) $n_1 = 1$, indicating that losses due to the bulk plasmon are expected when the metal forms a connected medium.

Associated to the deviation of the actual dipolar mode positions from the MG results is the appearance of non-negligible multipolar mode strengths, B_ν ($\nu = 2, ...$) and C_ν ($\nu = 2, ...$), and, accordingly (see Eqs. (3) and (5)), a reduction in the dipolar mode strengths B_1 and C_1. These mode strengths determine the dipolar peak heights in $\mathrm{Im}\left[\epsilon_{\mathrm{eff}}(\omega)\right]$ and $\mathrm{Im}\left[-\epsilon_{\mathrm{eff}}^{-1}(\omega)\right]$, represented in the inset of Fig. 6 as a function of f. For $B_1 = C_1 = 1$, all multipolar mode strengths being neglected, the dipolar peak heights in $\mathrm{Im}\left[\epsilon_{\mathrm{eff}}(\omega)\right]$ and $\mathrm{Im}\left[-\epsilon_{\mathrm{eff}}^{-1}(\omega)\right]$ are found to be $f\,H/\sqrt{m_1}$ and $f\,H/\sqrt{n_1}$, respectively, where H represents the peak height in the bulk energy-loss function (in the case of the Drude dielectric function of Eq. (13), $H = \omega_p/\gamma$). The actual dipolar peak heights divided by $f\,H$ are represented by stars and dots, together with the $B_1 = C_1 = 1$ approximation, i.e., $1/\sqrt{m_1}$ and $1/\sqrt{n_1}$, showing, therefore, the magnitude of the actual dipolar mode strengths involved in the spectral representations of Eqs. (1) and (4).

In summary, we have evaluated, on the basis of photonic band structure calculations, the effective long-wavelength dielectric response function of a system of long metallic cylinders. We have considered a spectral representation of both direct and inverse effective dielectric functions, of interest in the interpretation of absorption spectra and electron energy-loss experiments, respectively. We have analyzed the surface mode strengths and positions, and the effect of the electromagnetic interactions between the cylinders has been investigated. We have concluded that MG results are good as long as the distance between the axis of neighbouring cylinders is larger than twice the diameter of the cylinders. This is in contrast with the results we have also obtained for long dielectric cylinders. In this case we have found the MG results to be good for almost all the filling ratios for which the cylinders are not touching, as happens in the case of a periodic array of dielectric spheres[16].

ACKNOWLEDGMENTS

J. M. P. acknowledges partial support by the University of the Basque Country and the Basque Unibertsitate eta Ikerketa Saila under contracts UPV063.310EA056/96 and GV063.310-0017/95, respectively, and, also, by the British Council.

REFERENCES

[1] See, e.g., D. J. Bergman and D. Stroud, in Solid State Physics (H. Ehrenreich and D. Turnbull, eds.), Vol. 46, p. 147, Academic Press, New York (1992), and references therein.

[2] See, e.g., R. Landauer, in Electrical Transport and Optical Properties of Inhomogeneous Media, edited by J. C. Garland and D. B. Tanner, AIP Conf. Proc. No. 40 (AIP, New York, 1978), pp. 2-45.

[3] P. M. Echenique, J. Bausells, and A. Rivacoba, Phys. Rev. B **35**, 1521 (1987).

[4] C. Walsh, Philos. Mag. A **59**, 227 (1989); A. Howie and C. A. Walsh, Microsc. Microanal. Microstruct. **2**, 171 (1991).

[5] D. W. McComb and A. Howie, Nucl. Instrum. Methods B **96**, 569 (1995).

[6] J. B. Pendry and L. Martín-Moreno, Phys. Rev. B **50**, 5062 (1994); L. Martín-Moreno and J. B. Pendry, Nucl. Instrum. Methods B **96**, 565 (1995).

[7] R. G. Barrera and R. Fuchs, Phys. Rev. B **52**, 3256 (1995).

[8] R. Fuchs, R. G. Barrera, and J. L. Carrillo, Phys. Rev. B **54**, 12824 (1996).

[9] J. M. Pitarke, J. B. Pendry, and P. M. Echenique, Phys. Rev. B **55**, 9550 (1997).

[10] J. C. Maxwell-Garnett, Philos. Trans. R. Soc. London **203**, 385 (1904); **205**, 237 (1906).

[11] D. M. Wood and N. W. Ashcroft, Philos. Mag. **35**, 269 (1977).

[12] R. C. McPhedran and D. R. McKenzie, Proc. R. Soc. London A **359**, 45 (1978).

[13] W. Lamb, D. M. Wood, and N. W. Ascroft, Phys. Rev. B **21**, 2248 (1980).

[14] R. Tao, Z. Chen, and P. Sheng, Phys. Rev. B **41**, 2417 (1990).

[15] D. J. Bergman and K. J. Dunn, Phys. Rev. B **45**, 13262 (1992).

[16] S. Datta, C. T. Chan, K. M. Ho, and C. M. Soukoulis, Phys. Rev. B **48**, 14936 (1993).

[17] S. Ijima, Nature **354**, 56 (1991).

[18] L. A. Bursill, P. A. Stadelmannm J. L. Peng, and S. Prawer, Phys. Rev. B **49**, 1882 (1994).

[19] F. J. García-Vidal, J. M. Pitarke, and J. B. Pendry, Phys. Rev. Lett. **78**, 4289 (1997).

[20] J. B. Pendry and A. MacKinnon, Phys. Rev. Lett. **69**, 2772 (1992); J. B. Pendry, J. Mod. Opt. **41**, 2417 (1994); P. M. Bell, J. B. Pendry, L. Martín-Moreno, and A. J. Ward, Comput. Phys. Commun. **85**, 306 (1995).

[21] D. Bergman, Phys. Rep. **43**, 377 (1978).

[22] G. Milton, J. Appl. Phys. **52**, 5286 (1981).

[23] This spectral representation has been extended to the finite wavelength effective inverse longitudinal dielectric function of a system of spherical inclusions distributed at random within an otherwise homogeneous matrix (see Ref. 7) and, also, to the finite wavelength effective inverse longitudinal dielectric function of isolated cylinders (see Ref. 29).

[24] It is not necessary that the cylinders are circular, and the same result is found in the case of plane parallel layers aligned along the electric field. See, e.g., Ref. 1.

[25] See, e.g., C. F. Bohren and D. R. Huffman, *Absorption and Scattering of light by Small Particles* (Wiley, New York, 1983).

[26] R. G. Barrera, G. Monsivais, and W. L. Mochán, Phys. Rev. B, **38**, 5371 (1988); R. G. Barrera, J. Giraldo, and W. L. Mochán, Phys. Rev. B, **47**, 8528 (1993).

[27] F. J. García-Vidal and J. B. Pendry, Phys. Rev. Lett. **77**, 1163 (1996).

[28] Although for dielectric structures sampling meshes of $20 \times 1 \times 20$ have been found to provide well-converged results (see. e.g., Ref. 20), in the case of metallic inclusions in which the periodic structure has high dielectric contrast more dense meshes are needed for convergence.

[29] J. M. Pitarke and A. Rivacoba, Surf. Sci. **377**, 294 (1997).

[30] Experimental valence-loss spectra are usually acquired by using an effective collection angle, and this might result in a lower value of the largest transferred wavevector, q_c.

[31] For filling fractions as large as $x = 1.0$ and $x = 1.07$, the radius of the cylinders might need to be well below 1nm. For instance, it can be concluded from the calculations presented in Ref. 7 that for a system of spherical inclusions distributed at random within an otherwise homogeneous matrix the bulk plasmon excitation can be neglected for all filling fractions with $x \geq 1$, as long as the radius of the spheres is $a < 0.5$nm.

[32] In the long-wavelength limit, longitudinal and transverse dielectric functions with the same polarization coincide.

FIGURES

FIG. 1. Periodic array of metallic cylinders of diameter d arranged in a square array with lattice constant a. The cylinders are infinitely long in the y-direction.

FIG. 2. The imaginary part of the effective long-wavelength dielectric function of the periodic system described in Fig. 1, for p polarized electromagnetic excitations. Full thin line: the isolated cylinder result ($f \to 0$). Dotted, long-dashed, short-dashed, dashed-dotted and thick full lines: our numerical results for volume filling fractions of 2.2%, 19.6%, 54.5%, 68.6% and 74.0%, respectively.

FIG. 3. The same as in Fig. 2, for filling fractions of 54.5% and 74.0%. Full thin and thick lines: our numerical results. Dotted and dashed lines: MG results.

FIG. 4. The effective energy-loss function of the periodic system described in Fig. 1, for p polarized electromagnetic waves. Full thin line: the isolated cylinder result ($f \to 0$). Dotted, long-dashed, short-dashed, dashed-dotted and thick full lines: our numerical results for volume filling fractions of 2.2%, 19.6%, 54.5%, 68.6% and 78.5%, respectively. The bulk energy-loss function is represented bay a dotted line.

FIG. 5. The same as in Fig. 4, for filling fractions of 54.5% and 78.5%. Full thin and thick lines: our numerical results. Dotted and dashed lines: MG results.

FIG. 6. Dipolar mode positions (depolarization factors), as a function of the volume filling fraction f. Solid lines: our numerical results for m_1 (the line below the dilute limit of 1/2) and n_1 (the line above the dilute limit of 1/2). Dotted lines represent the MG depolarization factors given by Eqs. (10) and (11). Dipolar mode strengths are represented in the inset. Dots and stars: our numerical results for the dipolar peak heights in $\mathrm{Im}\left[\epsilon_{\mathrm{eff}}(\omega)\right]/(f\,H)$ and $\mathrm{Im}\left[-\epsilon_{\mathrm{eff}}^{-1}(\omega)\right]/(f\,H)$, respectively. Full thick and thin lines: $1/\sqrt{m_1}$ and $1/\sqrt{n_1}$, respectively. Here, $H = \omega_p/\gamma$.

Fig. 1

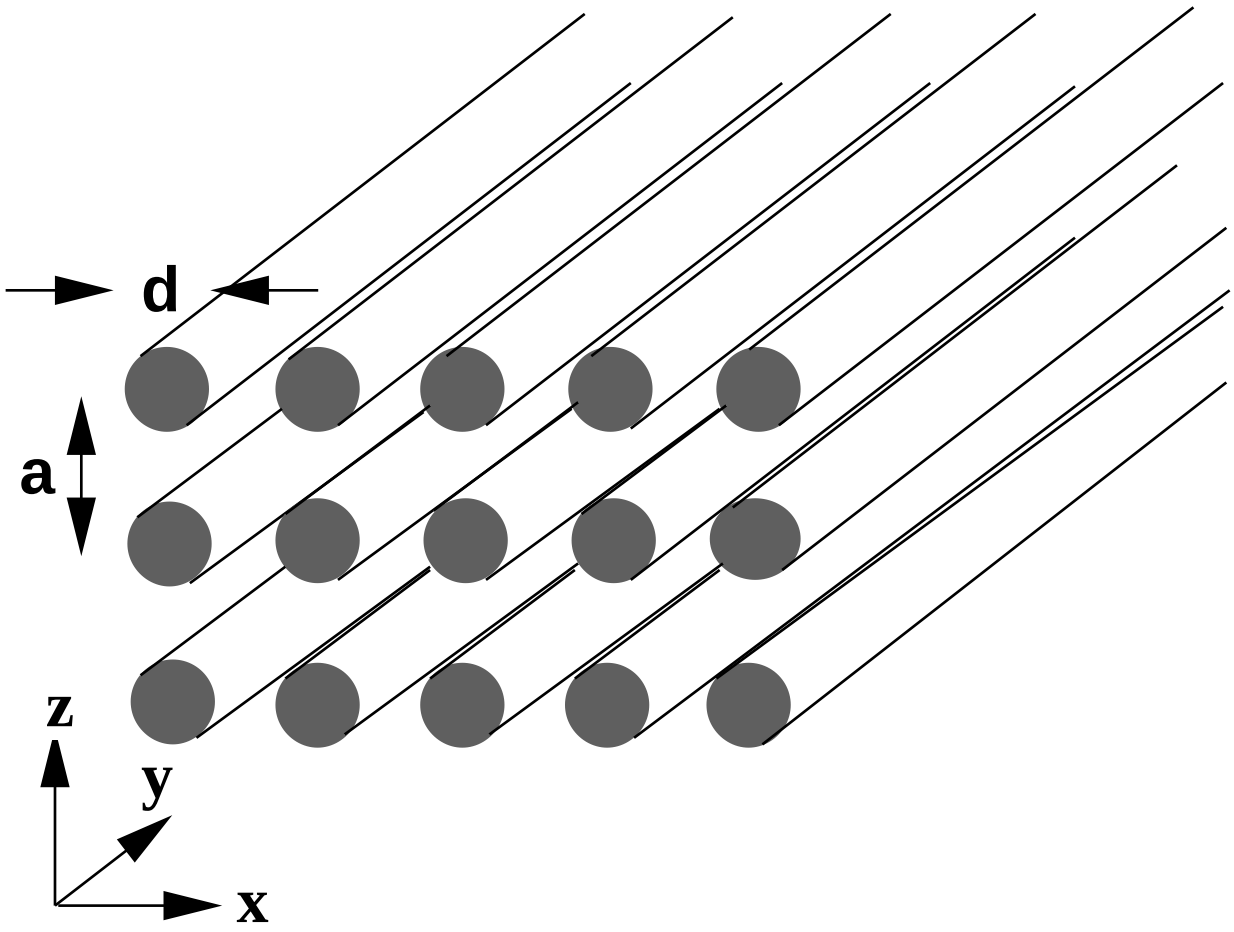

Fig. 2

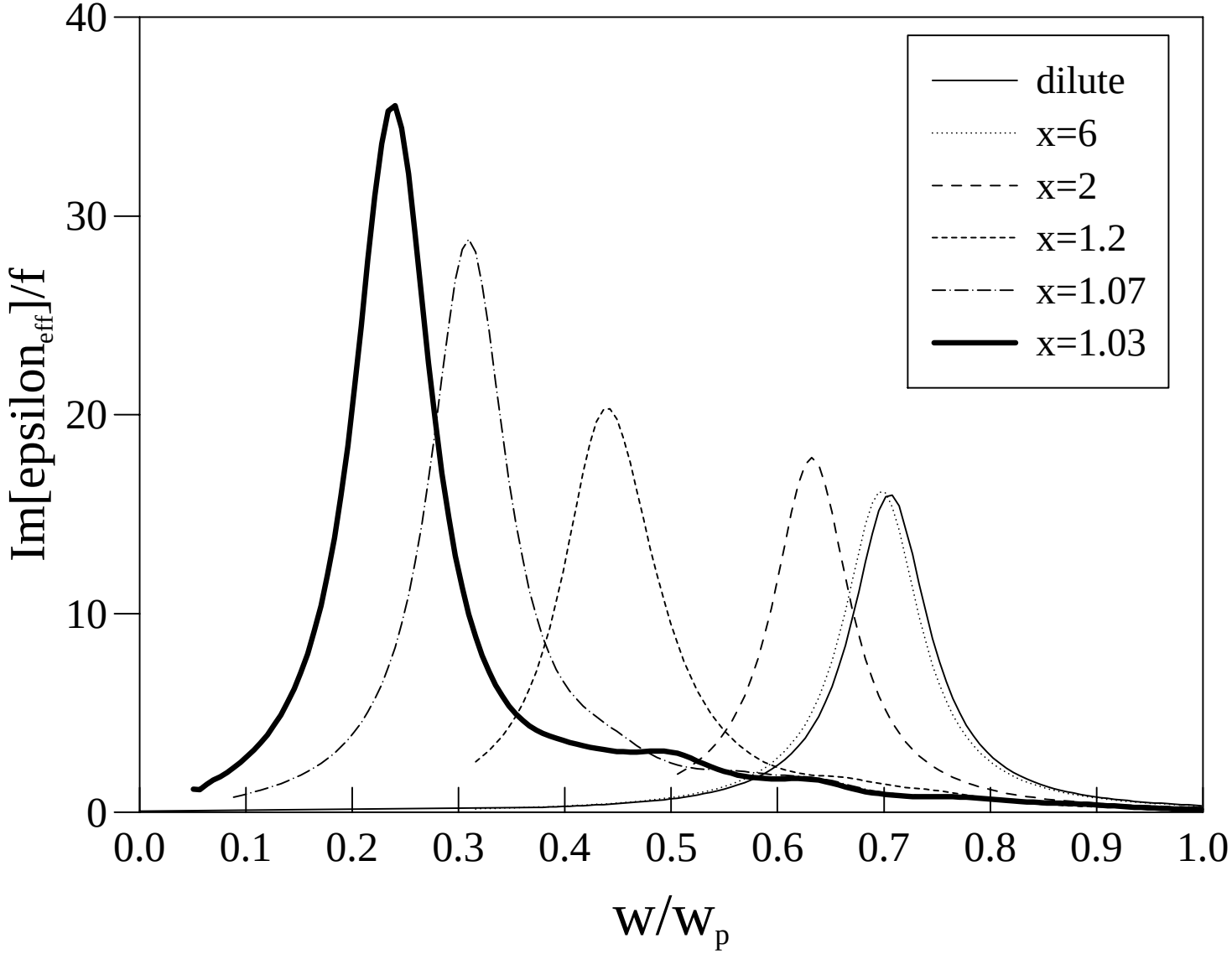
40
30
20
10
0
0.0
0.1
0.2
0.3
0.4
0.5
0.6
0.7
0.8
0.9
1.0
Im[epsilon$_{eff}$]/f
w/w$_p$
dilute
x=6
x=2
x=1.2
x=1.07
x=1.03

Fig. 3

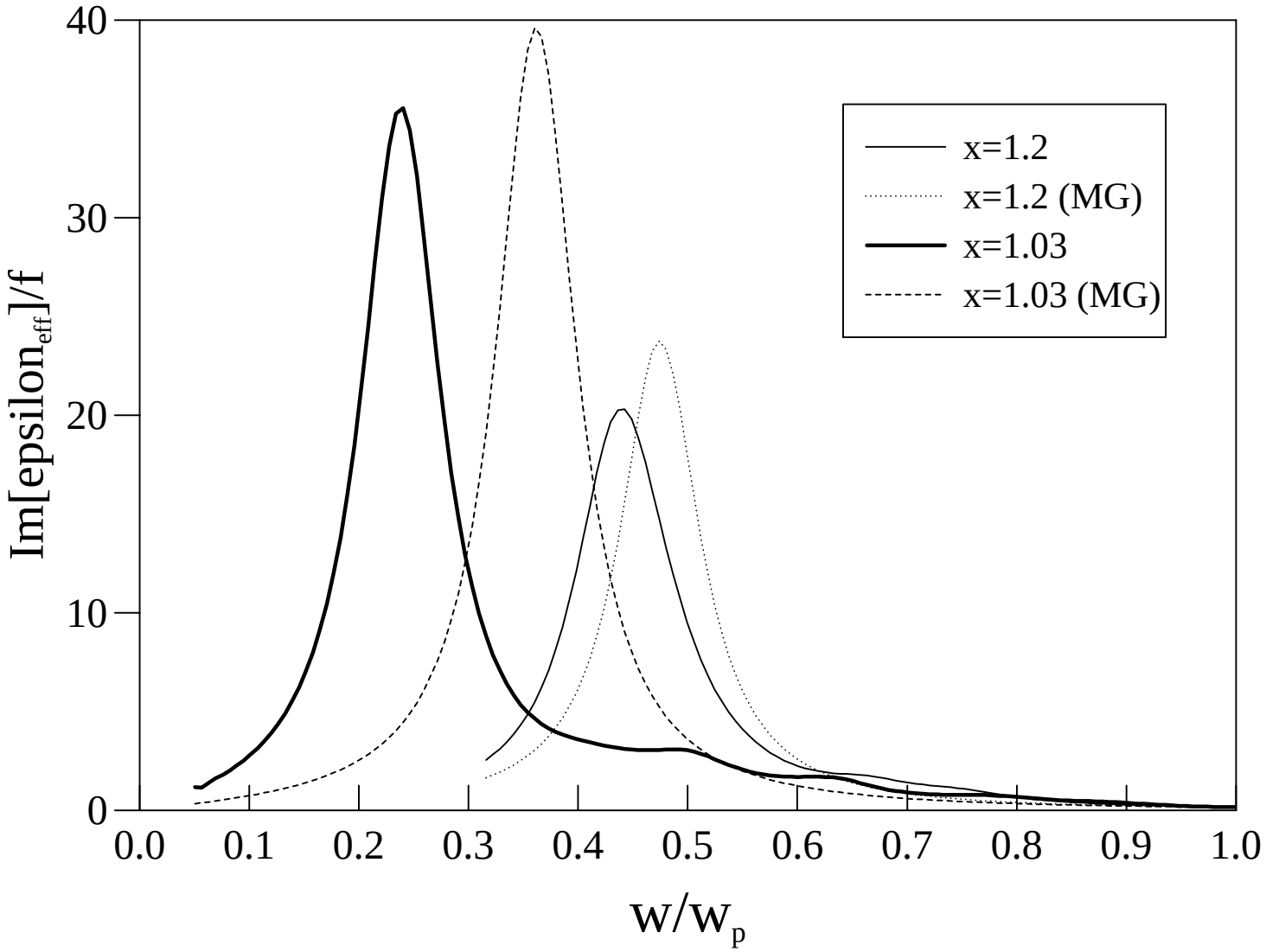
40
30
20
10
0
0.0
0.1
0.2
0.3
0.4
0.5
0.6
0.7
0.8
0.9
1.0
Im[epsilon_eff]/f
w/w_p
x=1.2
x=1.2 (MG)
x=1.03
x=1.03 (MG)

Fig. 4

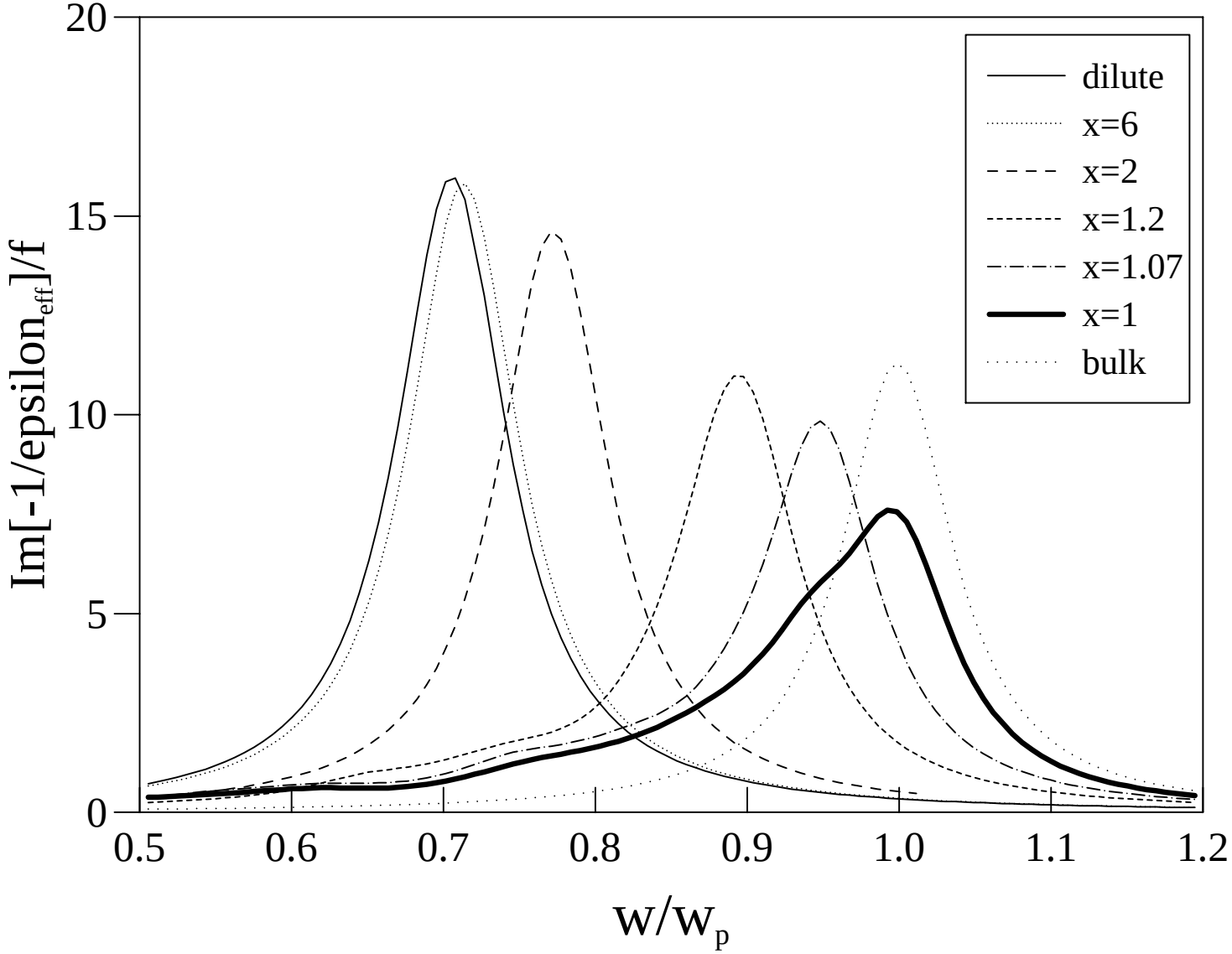
20
15
10
5
0
0.5
0.6
0.7
0.8
0.9
1.0
1.1
1.2
Im[-1/epsilon_eff]/f
w/w_p
dilute
x=6
x=2
x=1.2
x=1.07
x=1
bulk

Fig. 5

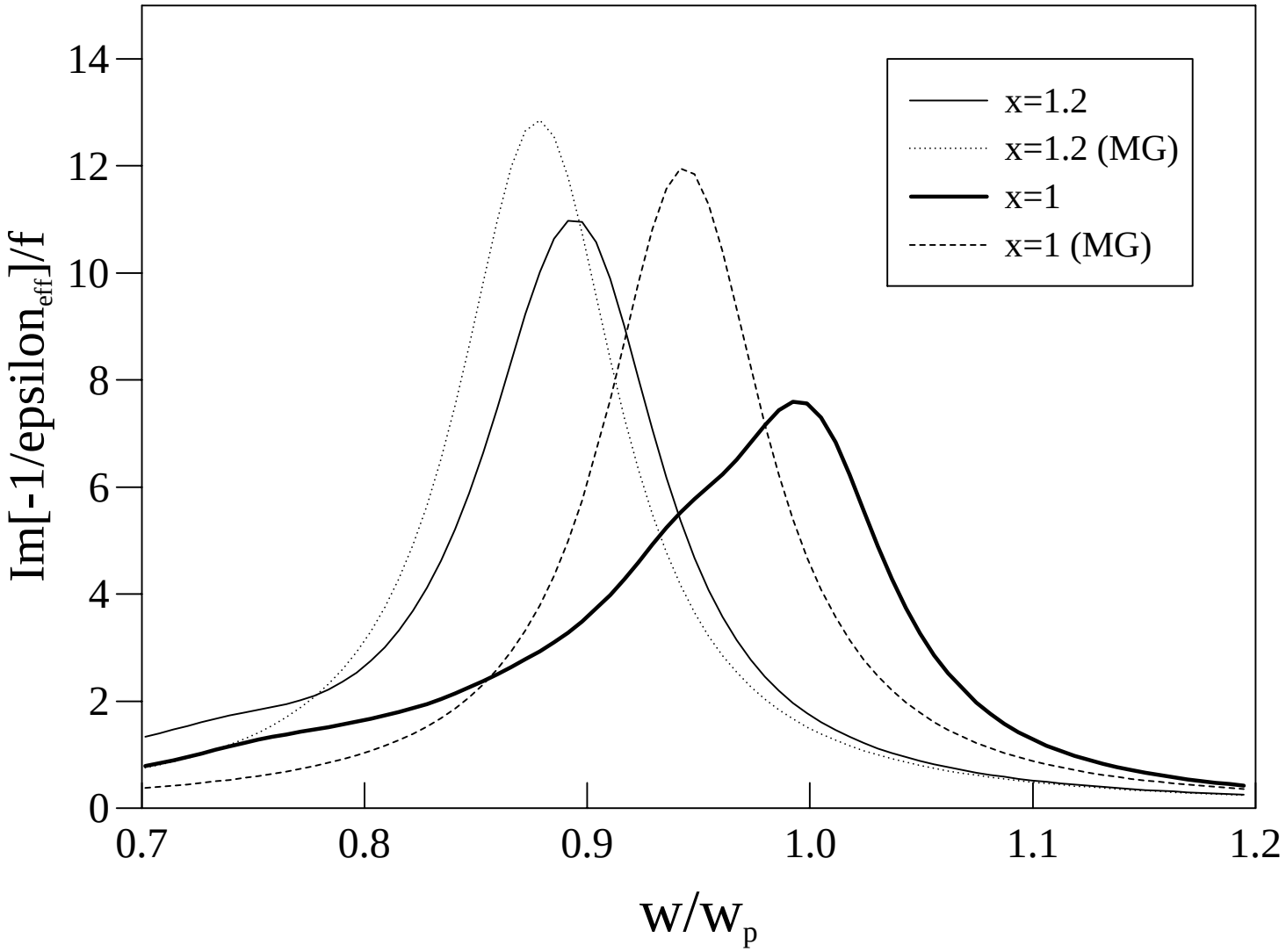
14
12
10
8
6
4
2
0
0.7
0.8
0.9
1.0
1.1
1.2
Im[-1/epsilon_eff]/f
w/w_p
x=1.2
x=1.2 (MG)
x=1
x=1 (MG)
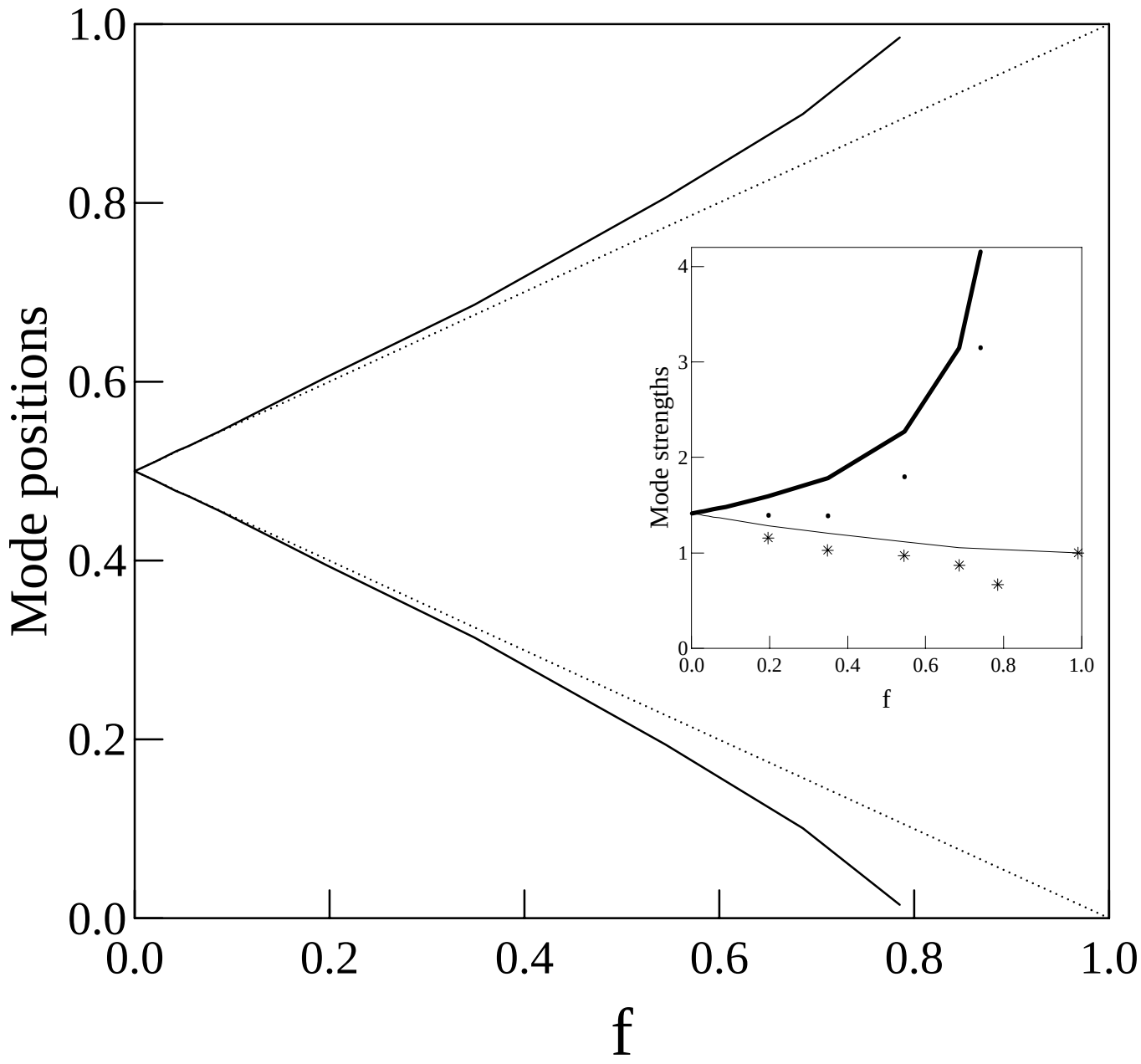
Fig. 6